Journal of Computers Vol. 32 No. 4, 2021, pp. 42-56
doi:10.53106/199115992021083204004

A Novel Denoising Algorithm of RFID Label Image Based on Singular Spectrum Analysis of Phase Space Reconstruction

Shanhao Zhou[1], Xiaolei Yu[2*], Ke Zhang[1], Zhenlu Liu[1], Lin Li[1], Zhimin Zhao[1]

[1] College of Science, Nanjing University of Aeronautics and Astronautics, Nanjing 210016, People's Republic of China
nuaazhoushanhao@126.com, zk2nuaa001009@163.com, lzl4997@nuaa.edu.cn, nuaa_lilin@nuaa.edu.cn, zhaozhimin@nuaa.edu.cn

[2] National Quality Supervision and Testing Center for RFID Product (Jiangsu), Nanjing 210029, People's Republic of China
xiaoleiyu@126.com

Received 2 December 2020; Revised 26 March 2021; Accepted 22 April 2021

Abstract. RFID label image is often polluted by noise, which reduces the efficiency of feature recognition of RFID label geometric distribution and affects the subsequent optimization. Aiming at it, this paper highlights a denoising algorithm for RFID label image based on singular spectrum analysis of phase space reconstruction. First, RFID label image is transformed into some sequence signals. Second, the improved Cao algorithm and SSA algorithm is proposed to denoise image, moreover, the processed sequence signal is reconverted to get the denoising image. In the paper, the rules of choosing the percentage to eliminate eigenvectors in SSA and how to superimpose the grayscale matrix are stipulated to improve the denoising efficiency. Finally, this paper compares the proposed algorithm with three denoising algorithms on different RFID label images to verify the effectiveness of this algorithm. The *PSNR* of the proposed algorithm are at least 0.3 dB higher than other denoising algorithms and the *SSIM* of the proposed algorithm are basically similar as NLM. Specially in the RFID semi-physical simulation experimental platform, the average of the *SSIM* of the square labels is 0.002 higher than NLM. The experiments show that the proposed algorithm in this paper is superior to the current common algorithms.

Keywords: image denoising, improved Cao algorithm, phase space reconstruction, singular spectrum analysis

1 Introduction

Radio Frequency Identification (RFID) is a key technology in the automation and perception layer of IOT [1, 2]. With the increasing demand of the high frequency band of RFID technology, it becomes the main topic how to improve the recognition performance of multi-label RFID system. Generally, the recognition performance of label system depends on the geometric distribution of Multi-label [3]. To improve the recognition performance of the multi-label RFID system, it is one of the key issues to determining the geometric distribution of the multi-label system. However, the geometric distribution of labels is generally obtained by image, and noise is the main factor affecting the quality of images. Therefore, in order to solve the problem that image noise hinders the feature extraction of RFID label image and the subsequent performance optimization of multi-label, the denoising of RFID label image is deeply studied in this paper.

* Corresponding Author

The research on image denoising has a long history. There are many classical algorithms for image denoising, such as median filtering and arithmetic mean filtering. Arithmetic mean filtering replaces each pixel of a noisy image with the average of each pixel around it, because the average of the surrounding pixel is closer to the real value, so this method can be used to eliminate isolated noise points. Its deficiency is that it will lose details and blur the picture. The principle of median filtering is very similar to that of arithmetic mean filtering, instead of the average, it uses the median value of the surrounding pixel to replace each pixel in a noisy image, it can retain details more than arithmetic mean filtering. But the algorithm is not fine enough to maximize the retention of the effective components of the image. The current relatively advanced non-local mean (NLM) denoising algorithm [4] was studied by A. Budades in 2005, NLM uses kernel function to find out the correlation degree of different regions of the image to denoise the image, which has a good effect. And a new non-local mean denoising algorithm is proposed by changing the kernel function in 2019 [5], the denoising effect of improved NLM filter is significantly improved (according to *PSNR* and *SSIM*). Because the coefficient of NLM kernel function will change with the different image, there is still no reliable theory to determine the coefficient of kernel function.

In addition, the singular spectrum analysis of phase space reconstruction is widely used in one-dimensional signal denoising [6], it is mainly to decompose the sequence signal according to the embedding dimension. Through this way, each vector after decomposition will contain the characteristic information of the original signal: its size distribution shows the distribution of the original signal energy, and the proportion of its energy to the whole system. The advantage of singular spectrum analysis of phase space reconstruction is that it can effectively extract the original information of the system to achieve denoising effect and the calculation of coefficients has the definite theory. On the basis of this theory, Yu Bin et al designed the algorithm to denoise the multi-path of the DBS and RMS, the improvement degree of the signal after noise reduction is higher than denoising by db10 wavelet filter [7]; Moreover, Khazraei used of MCSSA (Monte Carlo Singular Spectrum Analysis) to improve the GPS confidence rate to reach a level of about 95% for the extraction of signals during 20 years [8]. The above two good experimental results also reversely verify the effectiveness of this algorithm.

However, at present, the singular spectrum analysis based on phase space reconstruction, as a mean to screen out useful information of signals, has not been studied in depth in the RFID label image denoising. The reason for this is that the algorithm cannot be directly applied to two-dimensional images, because it involves the modification of the front and end of the algorithm program. There is still a big gap in the current attempt to improve the algorithm, so a denoising algorithm for RFID label image based on singular spectrum analysis of phase space reconstruction is proposed in this paper to extend this method to the RFID label images.

The singular spectrum analysis method based on phase space reconstruction mainly includes two parts: phase space reconstruction [9] and SSA [10]. For phase space reconstruction, the delay time τ should be found at first. Then, the best embedding dimension m needed finding. Next the best embedding dimension is used to reconstruct phase space. The selection of m is very important, but the traditional method is still insufficient for the selection. Therefore, this paper uses the improved Cao algorithm [6] to calculate the best embedding dimension m so that the best embedding dimension can be obtained more objectively and accurately, which lays a solid foundation for subsequent processing.

The signal components after phase space reconstruction are processed by SSA algorithm based on τ and m, and the noisy sequence signals are reconstructed into noise-free signals to realize the image denoising. Each sequence signal is obtained by row-by-row or column-by-column decomposition of the pixel matrix of the image.

For RFID label images, only a very small number of eigenvalues (about 2) have large values by the above processing, and the others are very small. Generally, the large eigenvalues retain the original signal of the image. Owing to the large gap of eigenvalue size of RFID label image, it is very convenient to eliminate noise, this convenience becomes the main advantage of the algorithm processing RFID label images in this paper.

This paper proposes a RFID label image denoising method, and the standard of eliminating the eigenvalues are set which represent noise. Finally, the quality of denoising image is further improved by superposition of gray matrix of RFID label image.

In order to solve the problem that image noise hinders the feature extraction of RFID label image, and better optimize multi-label performance, this paper proposes a novel denoising algorithm of RFID label image based on singular spectrum analysis of phase space reconstruction. It is found that:

(1) The *PSNR* of the different label denoising graphs using the proposed algorithm are at least 0.3 dB higher than other denoising algorithms;

(2) The *SSIM* of the different label denoising graphs using the proposed algorithm are basically same as NLM;

(3) But the average of the *SSIM* of the square labels in the RFID semi-physical simulation experimental platform is 0.002 higher than NLM.

The arrangements for this paper are made as follows. The second portion specifically introduces the theory and designs the proposed denoising algorithm. The third part, the proposed algorithm is compared with the arithmetic average filter, median filter and improved NLM filter denoising method (by *PSNR* and *SSIM* [11, 12]) in the case of single label or multiple labels. Finally, the conclusion is given.

2 Theory and Algorithm Design

2.1 The Cao Algorithm

Phase space reconstruction is mainly completed by Cao algorithm, Cao algorithm calculates the variation of the distance between a sequence X(n) and its nearest adjacent points $X_n(n)$ under the condition that the embedding dimension is m (integer):

$$\begin{aligned} &\mathrm{a}(\mathrm{i},m)=\frac{\left\|\mathrm{X}_{\mathrm{i}}(m+1)-\mathrm{X}_{\mathrm{n}(\mathrm{i},m)}(m+1)\right\|}{\mathrm{X}_{\mathrm{i}}(m)-\mathrm{X}_{\mathrm{n}(\mathrm{i},m)}(m)}, \\ &\mathrm{i}=1,2,\cdots,N-m. \end{aligned} \tag{1}$$

Here, $\|\cdot\|$ is the maximum norm, i represents the reconstructed phase space vector ordinal number; $X_{n(i,m)}(m)$ is the vector closest to $X_i(m)$ at the maximum norm.

The transverse coordinate value of the first Minimum point of the sequence mutual information function is the required delay time τ. The mutual information function is shown as Eq (2):

$$I(\mathrm{X};\mathrm{Y})=\sum_{y\in \mathrm{Y}}\sum_{x\in \mathrm{X}}p(x,y)\log[\frac{p(x,y)}{p(x)p(y)}]. \tag{2}$$

Here, p is the joint probability distribution function corresponding to the elements in parentheses, and I (X; Y) is the mutual information function about τ.

Then $E(m)$ and $E_1(m)$ are obtained according to Eq (3):

$$\begin{cases} E(m)=\dfrac{\sum_{i=1}^{N-m\tau}\mathrm{a}(i,m)}{N-m\tau}, \\ E_1(m)=\dfrac{E(m+1)}{E(m)}. \end{cases} \tag{3}$$

The $E(m)$ in the formula is the mean of the $a_{(i,m)}$ under the same embedding dimension; $E_1(m)$ is used as a reference to measure the trend of change of m. The $E_1(m)$ converges as the m increases. If the $E_1(m)$ remains stable when m is greater than m_0(integer), the best embedding dimension is equal to m_0+1.

2.2 The Improved Cao Algorithm

Since the sequence signal is fluctuating in the actual situation, which leads to E_1(m) is not convergent in most cases, some improvements should be made on the Cao algorithm. In this paper, the improvement is the change of the judgment basis of embedding dimension m, which may help us select the minimum embedding dimension more accurately.

The method is changed to the following four steps:

(1) The difference Δ_i is found between adjacent E_1(i), $1 \leqq i \leqq N-1$.

(2) The initial value of the threshold e (= 0.1) is set, and then the first subscript value i is found which satisfies $\Delta_i < e$.

(3) The new threshold $e = \overline{MAX\ (\Delta_i)}$ is set, $n \le i \le N-1$.

If a subscript value i can make $\Delta_i > \Delta_{i+1}$ 、$\Delta_{i+1} > \Delta_{i+2}$ 、$\Delta_i < e$, the value i+1 is the best embedding dimension m.

2.3 Singular Spectrum Analysis (SSA)

According to the improved Cao algorithm, the trajectory matrix X is obtained through the best embedding dimension:

$$X = \begin{pmatrix} x_1 & x_2 & \cdots & x_{N-m+1} \\ x_2 & x_3 & \cdots & x_{N-m+2} \\ \vdots & \vdots & \ddots & \vdots \\ x_m & x_{m+1} & \cdots & x_N \end{pmatrix}. \quad \textbf{(4)}$$

The x_j represents the j element in the general sequence X(n), the N is the number of elements in the general sequence X(n), and the m is the best embedding dimension.

By SSA the eigenvalue λ_i and eigenvector u_i of $S=XX^T$ are calculated, the eigenvectors of the eigenvalues are arranged from large to small as u_1 、u_2 、… 、u_N. Eigenvectors u_h 、u_{h+1} 、… 、u_N (h>1) are eliminated according to the percentage (the sum of above eigenvalues to the sum of all eigenvalues). Then get matrix $U = (u_1, u_2, \ldots, u_N)$, $U_t = (u_1, u_2, \ldots, u_{h-1})$ and $V=U^TX$. Next U_t is got by zeroing the elements of the U from h to N rows. Finally, the matrix $rca=U_tV_t$.

As shown in Eq (5), the reconstructed sequence is obtained.

$$y_k = \begin{cases} \dfrac{1}{k}\sum_{p=1}^{k} rca_{p,\,k-p+1},\ 1 \le k \le M^*, \\ \dfrac{1}{M^*}\sum_{p=1}^{M^*} rca_{p,\,k-p+1},\ M^* \le k \le K^*, \\ \dfrac{1}{N\text{-}k+1}\sum_{p=k-K^*+1}^{N-K^*+1} rca_{p,\,k-p+1},\ K^* \le k \le N, \\ K = N-m+1, \\ K^* = \max\{m, K\}, \\ M^* = \min\{m, K\}, \end{cases} \quad \textbf{(5)}$$

The $rca_{p,\,k-p+1}$ is the element of the rca, the m is the best embedding dimension obtained before, the N is the number of sequence signal elements. y_k is the element (k = 1, 2, …, N) of the reconstructed sequence, $Y_k = (y_1, y_2, \ldots, y_N)$.

2.4 The Proposed Denoising Algorithm

According to the Cao algorithm and SSA described above, the program flow chart of this algorithm is shown in Fig. 1.

There are three main improvements in this algorithm:

First, this paper presents a method to decompose the gray matrix of RFID label image row by row or column by column, which provides a means for the algorithm to be applied to RFID label image.

If the pixel matrix of the image H defined as follows:

$$H = \begin{pmatrix} x_{11} & x_{12} & \cdots & x_{1M} \\ x_{21} & x_{22} & \cdots & x_{2M} \\ \vdots & \vdots & \ddots & \vdots \\ x_{K1} & x_{K2} & \cdots & x_{KM} \end{pmatrix}. \quad \textbf{(6)}$$

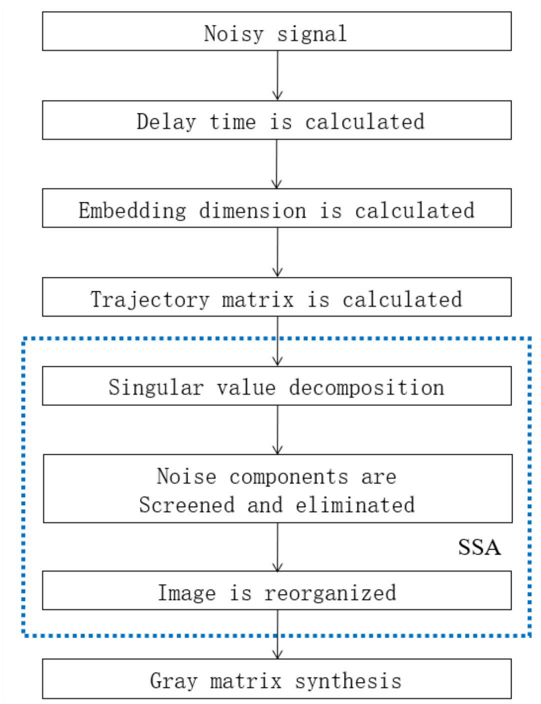

Fig. 1. Algorithm flow chart

The pixel matrix of a RFID image is decomposed line by line to obtain the general formula of K sequences as follows:

$$\begin{aligned} &\mathrm{r}_k = (x_{k1} \quad x_{k2} \quad \cdots \quad x_{kM}), \\ &k = 1, 2, \cdots K. \end{aligned} \qquad \textbf{(7)}$$

After substituting the K sequences into the algorithm in turn, these sequences are recombined into the image formula as follows:

$$E_x = \begin{pmatrix} Y_1' \\ Y_2' \\ \vdots \\ Y_K' \end{pmatrix}. \qquad \textbf{(8)}$$

Y'_1, Y'_2, …, Y'_K is the reconstructed sequence obtained by line-by-line substitution algorithm.

The pixel matrix of a RFID image is decomposed column by column to obtain the general formula of M sequences as follows:

$$\begin{aligned} &\mathrm{h}_k = (x_{1k} \quad x_{2k} \quad \cdots \quad x_{Kk}), \\ &k = 1, 2, \cdots M. \end{aligned} \qquad \textbf{(9)}$$

Y''_1, Y''_2, …, Y''_M is the reconstructed sequence obtained by column-by-column substitution algorithm

After substituting the M sequences into the algorithm in turn, these sequences are recombined into the image as follows:

$$E_{\mathrm{y}} = (Y_1^{''T} \quad Y_2^{''T} \quad \cdots \quad Y_M^{''T}). \qquad \textbf{(10)}$$

Secondly, for the eigenvalues of the RFID label image obtained from the SSA, it is found that the sum of the first two eigenvalues generally accounts for more than 95% of the sum of all eigenvalues, so the percentage used to eliminate eigenvectors u_h 、 u_{h+1} 、 … 、 u_N ($h > 1$) is set to 5%.

Thirdly, the superposition of the grayscale matrix is applied as a back-end processing algorithm proposed in this study to improve the image quality of denoising. The noise-containing images are respectively processed by the row-by-row and the column-by-column decomposition algorithm to obtain two image gray matrices. Furthermore, half of each gray matrix is superposed to obtain a final image, which will be detailed in the next section:

$$E' = \frac{1}{2}E_x + \frac{1}{2}E_y. \tag{11}$$

The E_x is the pixel matrix of the image after row-by-row algorithm processing, E_y is the pixel matrix of the image after column-by-column algorithm processing.

3 Experiment and Analysis

3.1 Single Label Image Denoising

In order to study the validity and robustness of the algorithm, the algorithm is used to for the long label and the round label images (single label). The effect is shown respectively in Fig. 2 and Fig. 3.

The first step is to add white Gaussian noise with a variance of 36 to a RFID label image, and then compare the image processed by phase space reconstruction algorithm and SSA with the original image to investigate the denoising effect of the algorithm. In the experiment, it is found that if the noise-containing images are only processed by the row-by-row or the column-by-column decomposition algorithm, the grayscale matrix reconstructed would have lots of stripes as shown in Fig. 2(c), Fig. 2(d), Fig. 3(c) and Fig. 3(d), for that the rows or columns of each input is unrelated.

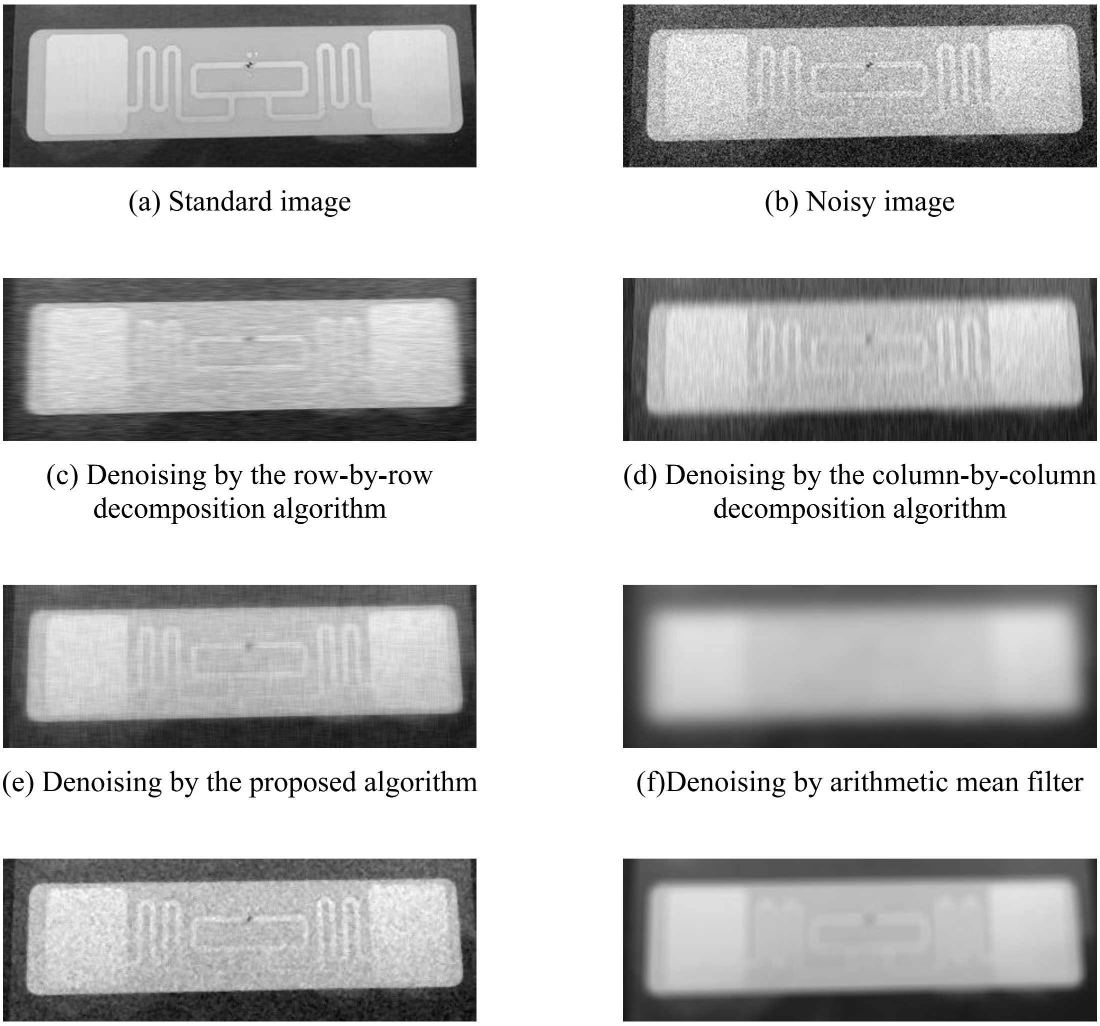

(a) Standard image

(b) Noisy image

(c) Denoising by the row-by-row decomposition algorithm

(d) Denoising by the column-by-column decomposition algorithm

(e) Denoising by the proposed algorithm

(f)Denoising by arithmetic mean filter

(g) Denoising by median filter

(h) Denoising by NLM filter

Fig. 2. Comparison of the denoising effect of the long label (single label)

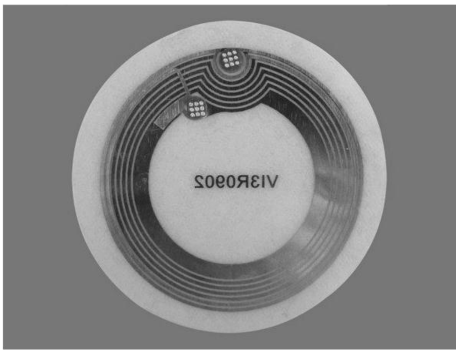

(a) Standard image

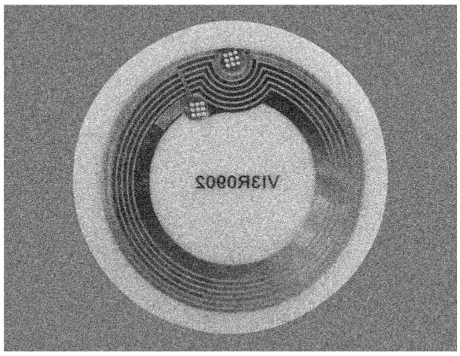

(b) Noisy image

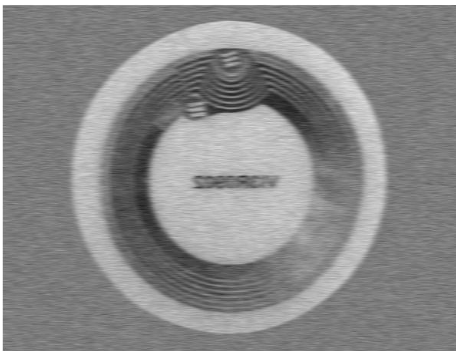

(c) Denoising by the row-by-row decomposition algorithm

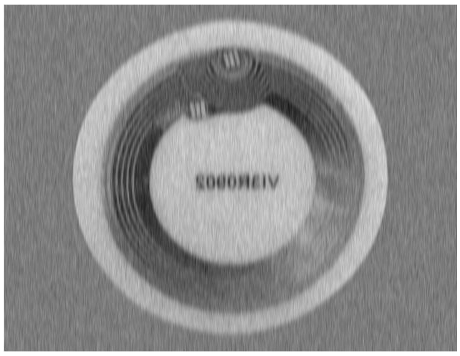

(d) Denoising by the column-by-column decomposition algorithm

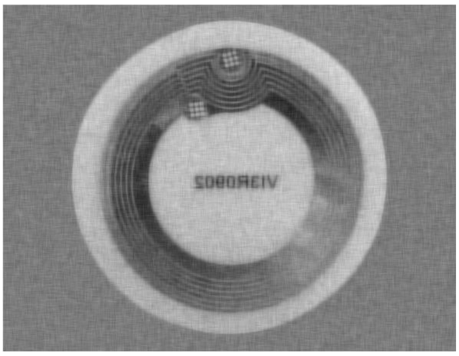

(e) Denoising by the proposed algorithm

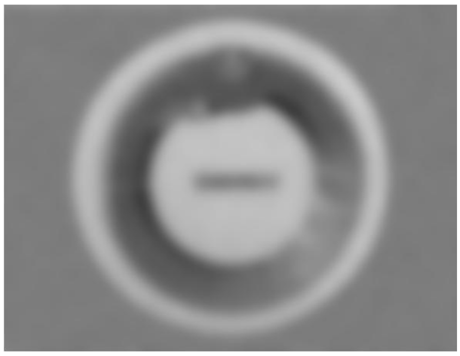

(f) Denoising by arithmetic mean filter

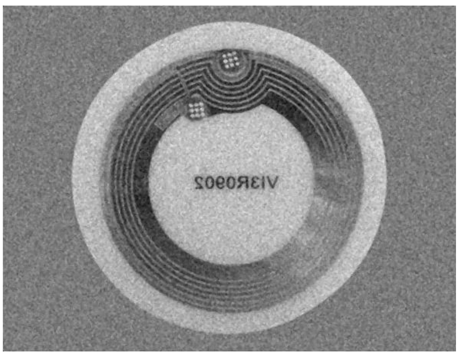

(g) Denoising by median filter

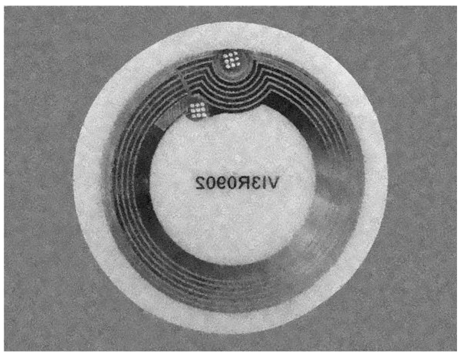

(h) Denoising by NLM filter

Fig. 3. Comparison of the denoising effect of the round label (single label)

For solving this problem, superposing half of the two image grayscale matrices reconstructed by line-by-line and column-by-column substitution algorithm to obtain a final image. The results show that the denoising effect is improved obviously after this processing, and the work of measuring image denoising quality by specific evaluation criteria will be elaborated in the next chapter.

The denoising effect of the improved algorithm, arithmetic mean filter, median filter and improved NLM filter are shown in Fig. 2(e), Fig. 2(f), Fig. 2(g), Fig. 2(h), Fig. 3(e), Fig. 2(f), Fig. 2(g), and Fig. 2(h), respectively. It can be seen from Fig. 2 : although the arithmetic mean filter can eliminate the noise, the denoising image got is very fuzzy, the effect of median filter to remove white Gaussian noise is not ideal in itself, while the improved NLM filter and the proposed algorithm not only de-noised the white Gaussian noise, but also got good vision effect.

The experimental results show that the proposed denoising algorithm has the denoising effect for both long and round RFID label (both single label) visually, the quantified evaluation of the denoising effect of these two RFID label images under various denoising methods will be shown in the end of this chapter.

3.2 Multi-label Image Denoising

In order to further study the robustness of the algorithm, the proposed algorithm is used to analyze and study multi-label image. This paper mainly studies the long strip multi-label image, and the effect is shown respectively in Fig. 4. According to the images, it is easy to get the same conclusion as the above experiment. The quantified evaluation of the denoising effect of the Multi-label image under various denoising methods will be shown in the end of this chapter.

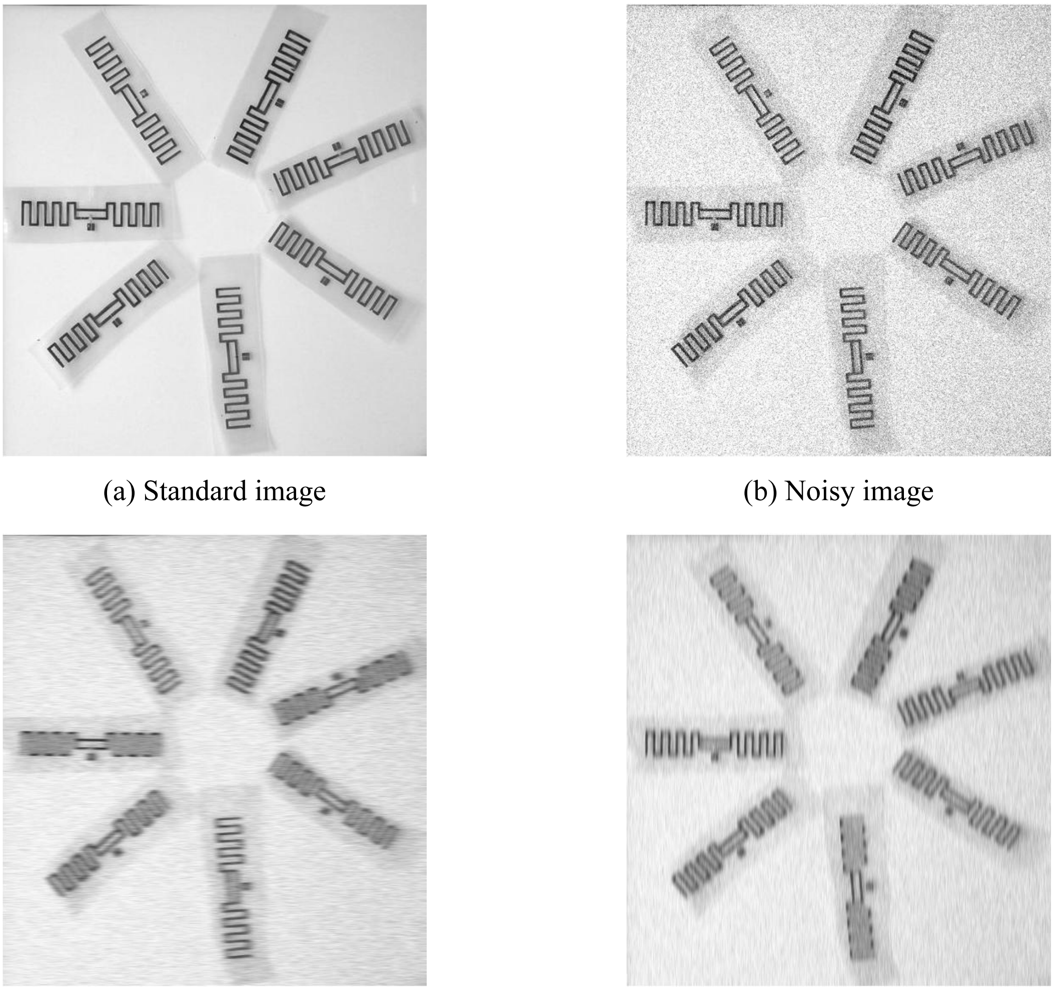

(a) Standard image

(b) Noisy image

(c) Denoising by the row-by-row decomposition algorithm

(d) Denoising by the column-by-column decomposition algorithm

Fig. 4. Comparison of the denoising effect of the long label (multi labels)

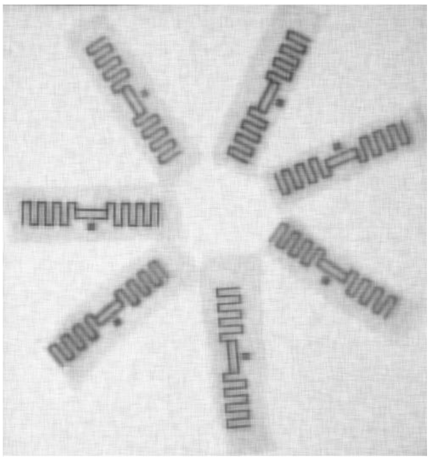

(e) Denoising by the proposed algorithm

(f) Denoising by arithmetic meanfilter

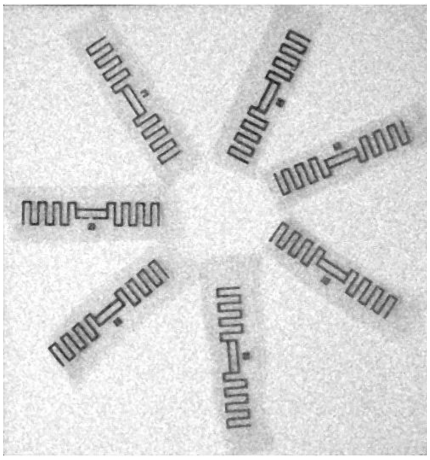

(g) Denoising by median filter

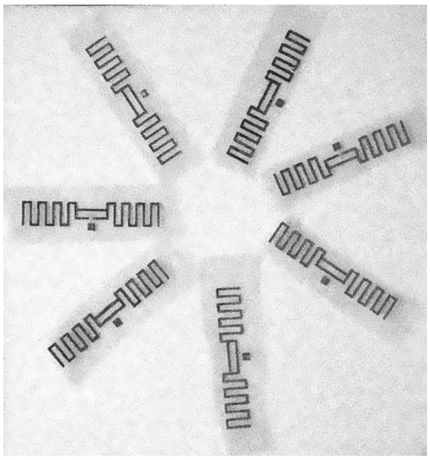

(h) Denoising by NLM filter

Fig. 4. Comparison of the denoising effect of the long label (multi labels) (continue)

3.3 The Label Denoising in The RFID Semi-physical Simulation Experimental Platform

In this paper, the denoising performance of the proposed algorithm is studied for the RFID labels in the RFID semi-physical simulation experimental platform and its feasibility is verified, which is intended to improve the recognition efficiency of the whole RFID label system by reducing the noise of the label image.

The denoising image of the square labels is carried out, and the hardware system used is the RFID semi-physical simulation experimental platform [3]. The RFID semi-physical simulation experimental platform imulates the operation of the system at the physical level, making the research process closer to the reality than other experiments. Because the research in this paper is to improve the quality of the image ingested by the RFID system, the image ingesting system is only introduced here. The hardware system of the RFID semi-physical simulation experimental platform is shown in Fig. 5(a).

The image acquisition system of this RFID system is composed of two cameras, labels, trestle and round chassis. The structure is shown in Fig. 5(b). Camera A and camera B shoot multiple labels from different angles, the image processed in this paper is the image taken by camera A.

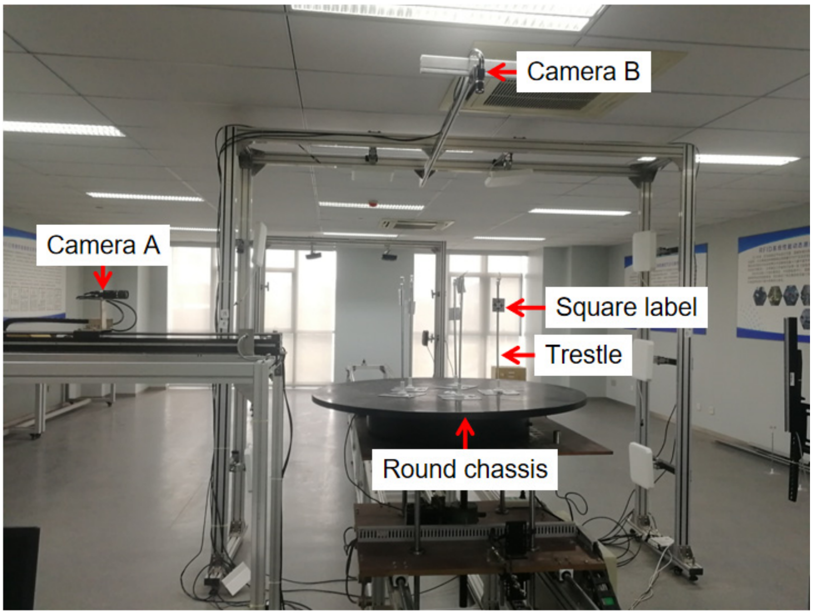

(a) Image of the designed real system based on the RFID semi-physical simulation experimental platform

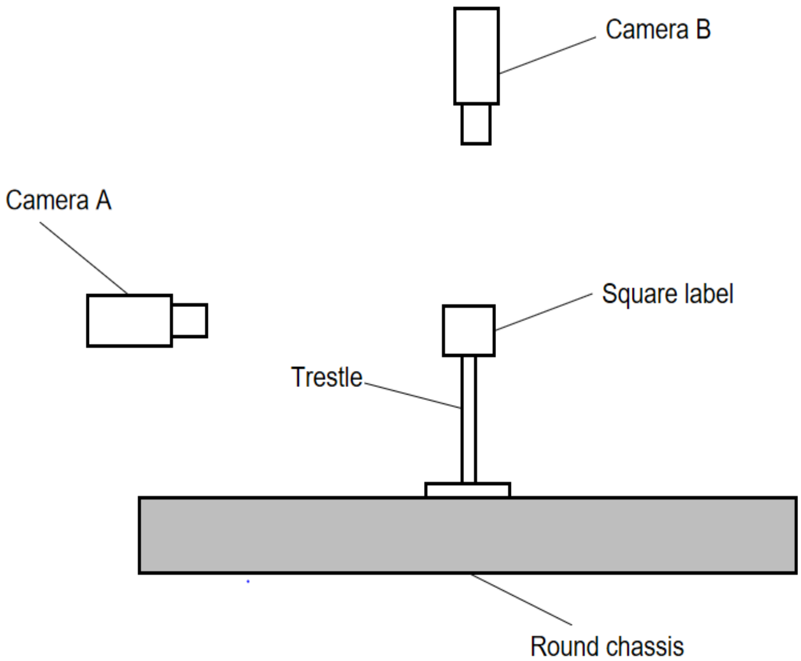

(b)The structure diagram of the system

Fig. 5. The hardware system display diagram

The image ingested by the system in the ideal state is shown in Fig. 6(a). However, Noise may be generated due to thermal and electromagnetic interference in the actual environment. In this paper, the image is added the same Gaussian white noise to simulate the environment under thermal and electromagnetic interference.

The results are shown in Fig. 6. According to the images, it can also get the same conclusion as the above experiments. The quantified evaluation of the denoising effect of the RFID labels in the RFID semi-physical simulation experimental platform under various denoising methods will be shown in the end of this chapter.

(a) Standard image

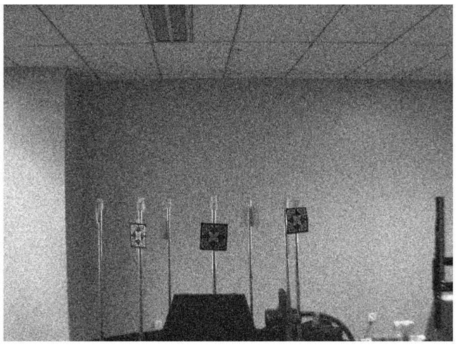

(b) Noisy image

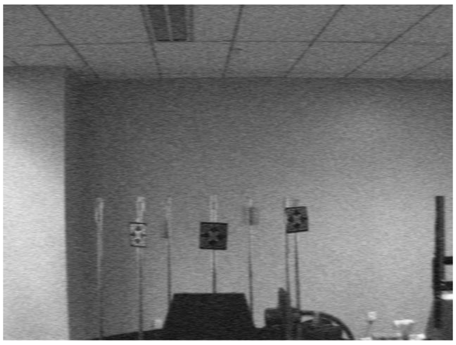

(c) Denoising by the row-by-row decomposition algorithm

(d) Denoising by the column-by-column decomposition algorithm

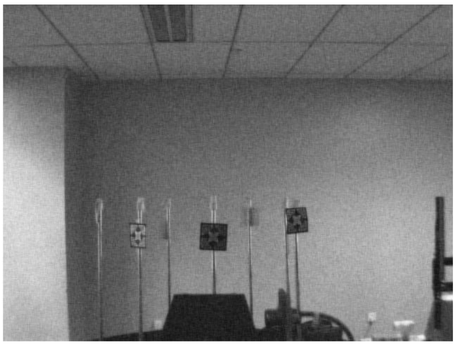

(e) Denoising by the proposed algorithm

(f) Denoising by arithmetic mean filter

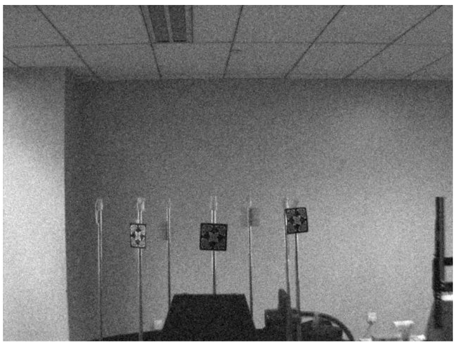

(g) Denoising by median filter

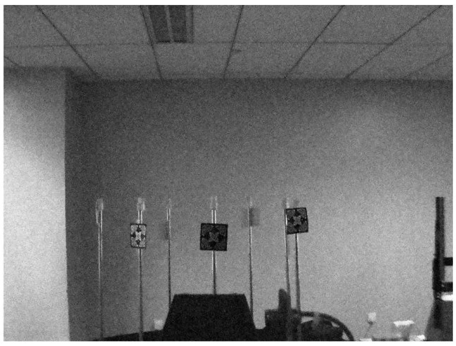

(h) Denoising by NLM filter

Fig. 6. Comparison of the denoising effect of the square labels

At the same time, the images are also studied which taken by the system under the other five different label distributions, as shown in Fig. 7, The quantified evaluation of the five results under various denoising methods will be shown in the end of this chapter.

(a) Random scene 1

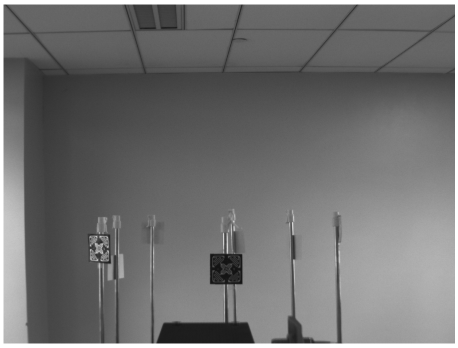

(b) Random scene 2

(c) Random scene 3

(d) Random scene 4

(e) Random scene 5

Fig. 7. Images captured under different label distributions

PSNR and *SSIM* are mainly used as two image quantization indicators to evaluate the quality of RFID label images after denoising. The peak signal-to-noise ratio (*PSNR*) is the ratio of the signal maximum power to the noise power, most people now think that it is more appropriate to evaluate the quality of the image than *SNR*. The *PSNR* is obtained by Eq 12:

$$PSNR = 10\log(\frac{255^2}{MSE}). \quad \textbf{(12)}$$

The MSE is the mean square error between the clear graph and the processing graph. At present, *PSNR* is widely used in the evaluation of the image quality, but it will not be proportional to the visual effect of the image, so it needs to be combined with the vision to evaluate the denoising effect.

SSIM is mainly used to evaluate the structural similarity of the image [10], by analyzing the three aspects: structure, contrast and brightness, which overcomes the limitation of the traditional SNR which cannot evaluate the image quality in all directions. The *SSIM* is between 0 and 1, the higher the value is, the more similar the two images are. The *SSIM* is obtained by Eq 13:

$$SSIM = \frac{(2\mu_x\mu_y + c_1)(2\sigma_{xy} + c_2)}{(\mu_x^2 + \mu_y^2 + c_1)(\sigma_x^2 + \sigma_y^2 + c_2)}. \quad \textbf{(13)}$$

x and y are the gray matrix elements of two images, where μ_x and μ_y are the averages as parameters for measuring brightness. σ^2_x and σ^2_y are variance, which is used as the parameter to measure contrast. σ_{xy} is the covariance of x and y, which is a parameter to measure the degree of structural similarity. $C_1 = (k_1L)^2$ and $c_2 = (k_2L)^2$ are constants for maintaining stability, L is the dynamic range of pixel values. General constants k_1 and k_2 are 0.01 and 0.03 respectively

The denoising effect of various algorithms is evaluated by *PSNR* and *SSIM*. The results are shown in Table 1 and Table 2. The values of *PSNR* and *SSIM* in the tables are the average calculation results of different label images after multiple runs in the same case.

Table 1. *PSNR* (dB) by denoising by various methods

Category	Median filter	Arithmetic mean filter	Improved NLM filter [5]	Row-by-row (Cao+SSA)	Column-by-column (Cao+SSA)	Our algorithm
Long label (Fig. 2)	26.13	26.25	26.67	27.28	25.79	28.24
Round label (Fig. 3)	26.11	24.29	25.50	25.73	25.57	26.41
Long labels (Fig. 4)	26.12	24.21	22.71	23.64	23.43	27.21
Square (Fig. 7)	26.71	27.76	29.57	27.98	28.99	29.91
Square (Fig. 8(a))	26.69	27.89	29.61	28.01	29.00	29.95
Square (Fig. 8(b))	26.75	27.78	29.54	27.95	28.93	29.99
Square (Fig. 8(c))	26.83	27.91	29.49	28.06	28.91	29.85
Square (Fig. 8(d))	26.65	27.84	29.57	27.99	28.93	29.88
Square (Fig. 8(e))	26.77	27.83	29.63	28.05	28.98	29.94
Average of square labels	26.73	27.84	29.57	28.01	28.96	29.92

Table 2. *SSIM* by denoising by various methods

Shape	Median filter	Arithmetic mean filter	Improved NLM filter [5]	Row-by-row (Cao+SSA)	Column-by-column (Cao+SSA)	Our algorithm
Long label (Fig. 2)	0.541	0.681	0.738	0.623	0.611	0.733
Round label (Fig. 3)	0.641	0.762	0.793	0.735	0.733	0.796
Long labels (Fig. 4)	0.645	0.784	0.816	0.770	0.771	0.826
Square (Fig. 7)	0.735	0.898	0.922	0.867	0.886	0.919
Square (Fig. 8(a))	0.736	0.902	0.918	0.871	0.889	0.920
Square (Fig. 8(b))	0.735	0.897	0.920	0.866	0.884	0.923
Square (Fig. 8(c))	0.733	0.900	0.915	0.863	0.879	0.918
Square (Fig. 8(d))	0.731	0.899	0.912	0.869	0.886	0.924
Square (Fig. 8(e))	0.740	0.897	0.920	0.874	0.881	0.915
Average of square labels	0.735	0.899	0.918	0.868	0.884	0.920

It can be seen in Table 1 that the *PSNR* of the algorithm proposed in this paper improved a lot compared with other algorithms, with the least increase of round single label (0.3 dB); and the most increase of long multi labels (4.5 dB).

As can be seen from Table 2, Compared with the two classical denoising methods (mean filter and median filter), the proposed algorithm still has an advantage. For long single label, it is 0.005 lower than improved NLM filter. However, for round single label and long multi labels, it is 0.003 and 0.001 higher than improved NLM filter respectively. The Average of the *SSIM* of six different label distribution images on a semi-physical simulation platform is 0.002 higher than improved NLM filter. In the mass, the proposed algorithm and the improved NLM filter are similar, but the proposed algorithm is slightly stronger.

Thus, it is feasible to use singular spectrum analysis based on phase space reconstruction to realize image denoising. According to the characteristics of the trajectory matrix obtained by RFID label image, this paper selects appropriate h to improve the utilization of useful components of the algorithm. Moreover, the method of image pixel matrix superposition makes up for the shortcomings of denoising image texture. Two improvements make the *PSNR* and *SSIM* of the algorithm much higher than the classical filters such as median filter and arithmetic mean filter. Though the *SSIM* advantage is not great, but it should be noted that *SSIM* is a quantitative index of image similarity, focusing on the visual perception of denoising images by human eyes. However, the *PSNR* is measured by the useful signal in the two-dimensional signal. The direct purpose of denoising in this paper is to improve the efficiency of feature extraction of label images by RFID system, and this feature extraction depends more on the recognition of useful signals (measured by *PSNR*). Therefore, this algorithm has a slight advantage over other algorithms mentioned in this paper.

4 Conclusion

This paper proposed phase space reconstruction and SSA to denoise the RFID label image. The *PSNR* of the different label denoising images by the proposed algorithm are at least 0.3 dB higher than other denoising algorithms. And the *SSIM* of the different label denoising images by the proposed algorithm are basically same as NLM. However, the average of the *SSIM* of the square labels in the RFID semi-physical simulation experimental platform is 0.002 higher than NLM, which shows that this algorithm has a slight advantage over other algorithms in application. In the overall, it can be proved that this algorithm is superior to the current common algorithms denoising effect of Gaussian white noise in RFID label image. The algorithm proposed in this paper lays a good foundation for the subsequent RFID label recognition based on the denoising label image.

The main deficiency of this algorithm is that the determination of h in SSA needs to be estimated by more sophisticated algorithms, just like the improvement of Cao algorithm. The further optimization of h is very important for the further improvement of robustness and denoising effect. In addition, the future research will be more in-depth in improving the denoising effect, the current idea is to achieve this goal by preprocessing the image pixel matrix (such as convolution with a two-dimensional discrete probability template).

Acknowledgements

The work was financially supported by the National Natural Science Foundation of China [61771240], China Postdoctoral Science Foundation [2016 T90452] and the Six Talent Peaks Project in Jiangsu Province of China [XYDXX-058].

References

[1] P. Solic, Z. Blazevic, M. Skiljo et al., Gen2 RFID as IoT Enabler: Characterization and Performance Improvement, IEEE Wireless Communications 24(3)(2017) 33-39.

[2] Malik Čabaravdić, Sanela Čančar, Anel Husaković, Application of Mini Computers and RFID Technology in Automation, Springer International Publishing, West Berlin and Heidelberg, 2018.

[3] X.-L. Yu, D. Wang, Z.-M. Zhao, Semi-physical Verification Technology for Dynamic Performance of Internet of Things System, Singapore:Springer, Springer, 2019.

[4] A. Budades, B. Coll, J.M. Morel, A Review of Image Denoising Algorithms, with A New One, Multiscale Modeling and Simulation 4(2)(2005) 490530.

[5] J. Xu, Y. Hao, Improved Weight Function for Nonlocal Means Image Denoising, Journal of Donghua University (Eng.Ed.), 035(005)(2018) 394-398.

[6] X. Zho, Y. Cui, L. Li et al., Signal De-noising in Gear Pitting Fault Identification by An Improved Singular Value Decomposition Method, Forschung Im Ingenieurwesen-engineering Research 84(2020) 79-90.

[7] B. Yu, S. Yang, Analysis of Singular Spectrum Based on Improved Cao Algorithm and its Application in Beidou Multipath Denoising Filtering, Journal of Geodesy and Geodynamics 39(01)(2019) 29-34.

[8] S.M. Khazraei, A.R. Amiri Simkooei, On the Application of Monte Carlo Singular Spectrum Analysis to GPS Position Time Series, Journal of Geodesy 93(9)(2019) 1401-1418.

[9] R. Bhavsar, N. Davey, N. Helian et al., Time Series Analysis Using Embedding Dimension on Heart Rate Variability, Procedia Computer Science 145(2018) 89-96.

[10] A.R. Khan, D.S. Poskitt, A Note on Window Length Selection in Singular Spectrum Analysis, Australian and New Zealand Journal of Statistics 55(2)(2013) 87- 108.

[11] U. Sara, M. Akter, M.S., Uddin Image Quality Assessment Through FSIM, SSIM, MSE and PSNR—A Comparative Study, Journal of Computer and Communications 07(3)(2019) 8-18.

[12] Alain Horé, D. Ziou, Image Quality Metrics: PSNR vs. SSIM, in: computer society, in: Proc. 2010 International Conference on Pattern Recognition, 2010.